Surface Modifications of Oil Palm Mesocarp Fiber by Superheated Steam, Alkali, and Superheated Steam-Alkali for Biocomposite Applications

Yoon Yee Then,[a] Nor Azowa Ibrahim,[a,*] Norhazlin Zainuddin,[a] Hidayah Ariffin,[b] Wan Md Zin Wan Yunus,[c] and Buong Woei Chieng [a]

In this work, surface modifications of oil palm mesocarp fiber were carried out by using superheated steam, alkali, and consecutive superheated steam-alkali treatments, aiming at modification of fiber's surface for biocomposite applications. The chemical compositions of fiber were modified after treatments as validated by chemical analysis and Fourier transform infrared spectroscopy. The treated fibers under microscopy observation showed relatively clean, rough, and textured surfaces due to the elimination of impurities and hemicellulose. The crystallinity index and thermal stability of treated fibers were relatively higher than that of untreated fiber as determined by X-ray diffraction and thermogravimetric analyses, respectively. A reduction in water absorption of fiber after treatments was also noted. These results indicated those treatments were effective in modifying the chemical compositions and microstructure of fiber. The treatments also increased the crystallinity and thermal stability, as well as reduced the hygroscopicity of fiber. Those treatments could increase the suitability of fiber to be used in the development of biocomposites.

Contact information: a: Department of Chemistry, Faculty of Science, Universiti Putra Malaysia, 43400 UPM Serdang, Selangor, Malaysia; b: Department of Bioprocess Technology, Faculty of Biotechnology and Biomolecular Sciences, Universiti Putra Malaysia, 43400 UPM Serdang, Selangor, Malaysia; c: Department of Chemistry, Centre For Defence Foundation Studies, National Defence University of Malaysia, Sungai Besi Camp, 57000 Kuala Lumpur, Federal Territory of Kuala Lumpur, Malaysia; * Corresponding author: norazowa@upm.edu.my

INTRODUCTION

Using natural fibers as potential substitution to synthetic fibers in biocomposite applications is of interest currently from the environmental point of view. These natural fibers are: renewable, biodegradable, easily available, light weight, and inexpensive. Thus they offer great opportunities in manufacturing of light weight yet eco-friendly biocomposites (Kalia *et al.* 2009). Natural fibers such as kenaf (Ibrahim *et al.* 2010; Ahmad Thirmizir *et al.* 2011; Abdul Razak *et al.* 2014), oil palm (Sreekala *et al.* 2000; Then *et al.* 2013; Teh *et al.* 2013; Rayung *et al.* 2014; Then *et al.* 2014), coir (Islam *et al.* 2010), henequen (Herrera-Franco and Valadez-Gonzalez 2005), and jute (Razera and Frollini 2004; Sinha and Rout 2009) have been used in manufacturing of biocomposites.

Oil palm mesocarp fiber (OPMF), a lignocellulose residue left behind in the palm oil mill has considerable potential to be used in biocomposite production due to its availability in large quantities in the palm oil industry (Sreekala *et al.* 1997). It was reported that the amount of OPMF generated in Malaysia in 2013 was 17.8 million tons

(GGS 2014). Currently, OPMF is used as low value boiler fuel to generate electricity for self supply of the palm oil mill (Lau *et al.* 2008). Thus, there is no doubt that the use of OPMF as filler to develop biocomposites will be an added value of OPMF in the future.

However, certain drawbacks of natural fibers, particularly the degradation during processing, poor wettability, and compatibility with hydrophobic thermoplastics as well as high moisture absorption behavior, make them unsuitable to be used in biocomposite fabrications (Kalia *et al.* 2009). These problems can be solved or minimized by modifying the surface of fibers, aiming at improving their adhesion characteristic toward hydrophobic thermoplastics as well as to reduce their moisture absorption characteristic. Recently various types of treatments have been carried out to modify the surface properties of fibers, including alkalization (Sreekala *et al.* 2000; Xiao *et al.* 2001; Mwaikambo and Ansell 2002; Herrera-Franco and Valadez-Gonzalez 2005; Mohd Edeerozey *et al.* 2007; John and Thomas 2008; Sinha and Rout 2009; Ibrahim *et al.* 2010; Saha *et al.* 2010), chemical grafting (Sreekala *et al.* 2000; Teh *et al.* 2013), chemical bleaching (Abdul Razak *et al.* 2014; Rayung *et al.* 2014) and steaming (Wang *et al.* 2009; Bahrin *et al.* 2012; Then *et al.* 2014). These treatments normally lead to reduction in moisture uptake, as well as changes in the fiber surface properties.

It is known that the primary attraction of biocomposites market nowadays is the competitive price of natural fibers. Therefore, low-cost and efficient modification processes for natural fibers are of importance in producing strong materials at a competitive price. In this work, alkali and superheated steam treatments were chosen because these treatments appear to be relatively simple and inexpensive but effective to modify the surface of fiber with least environmental impact (Xiao *et al.* 2001; Mwaikambo and Ansell 2002; Mohd Edeerozey *et al.* 2007; Bahrin *et al.* 2012; Then *et al.* 2014). It was reported that the alkali and superheated steam treatments can eliminate most of the impurities (waxy substances) present on the surface of fiber and part of the non-cellulose components (*e.g.* hemicellulose and lignin) (Mwaikambo and Ansell 2002; Bahrin *et al.* 2012; Then *et al.* 2014). The removal of these substances can increase the surface roughness of fiber, promoting the adhesion between thermoplastic and fiber, particularly via mechanical interlocking mechanism (Mohd Edeerozey *et al.* 2007). This could result in biocomposites with improved mechanical properties. Additionally, those treatments also can increase the thermal stability and crystallinity of fiber as reported by other researchers (Mwaikambo and Ansell 2002; Bahrin *et al.* 2012). As mentioned earlier, a single treatment process by alkali or superheated steam can only partially remove the non-cellulose components in fiber, and those remaining non-cellulose components can hinder the performance of the biocomposite fabricated. As consequences, combination treatments by superheated steam and alkali can be the solution to enhance the efficiency of non-cellulose components removal in fiber, which in turn can further enhance the biocomposites performance. The utilization of consecutive superheated steam-alkali treatment to modify the fiber surface properties has not been reported previously.

In the present work, we have investigated the influence of superheated steam, alkali, and consecutive superheated steam-alkali treatments on the properties of OPMF. The chemical compositions, morphological, structural, crystallinity, thermal degradation, and water absorption behaviors of treated fibers were investigated through chemical analysis, scanning electron microscopy, Fourier transform infrared spectroscopy, X-ray diffraction analysis, thermogravimetric analysis, and water absorption test. The main

purpose of these modification processes is to enhance the interfacial adhesion between hydrophilic natural fiber and hydrophobic thermoplastic in subsequent work.

EXPERIMENTAL

Materials
Oil palm mesocarp fiber (OPMF) was collected from FELDA Serting Hilir Palm Oil Mill, Malaysia. It was first washed by soaking in distilled water for 24 h then rinsed with hot water (60 ˚C) and finally with acetone prior to oven-drying at 60 ˚C for 24 h. This process aimed to remove dirt from the fiber surface. The dried fiber was then ground, sieved into particle size of 150 to 300 μm, and kept in a sealed polyethylene bag to be used in treatment processes. NaOH pellets, KOH pellets, and H_2SO_4 were purchased from Merck (Germany). Sodium chlorite ($NaClO_2$) was purchased from Acros Organics (Belgium). The NaOH, $NaClO_2$, H_2SO_4, and KOH are based on analytical grade and used as received.

Surface Modifications of Fiber
Prior to modification process, the untreated OPMF was oven-dried at 60 ˚C until constant weight was achieved.

Modification of OPMF by alkali treatment
The modification process was carried out according to the method described by Ibrahim *et al.* (2010). The dried OPMF was soaked in 5% NaOH solution for 3 h at room temperature. The weight ratio of OPMF to NaOH solution was fixed at 1:20. After the treatment, the fiber was filtered and washed several times with water then oven-dried at 60 ˚C and finally kept in a seal polyethylene bag for further used.

Modification of OPMF by superheated steam treatment
The modification process was carried out in a superheated steam oven, Model QF-5200C, under normal atmospheric pressure following the method described by Then *et al.* (2014). Regular tap water was used to produce the superheated steam. In brief, the temperature of superheated steam oven was first set to 220 ˚C and allowed to reach a steady state. Next, about 20 g of OPMF was uniformly poured on the aluminium foil tray ($10 \times 12 \times 1$ cm^3). It was then put into the heating chamber of superheated steam oven for 1 h. Once treatment completed, fiber was removed immediately from the heating chamber, cooled in a desiccator, and finally kept in the sealed polyethylene bag to be used in analysis.

Modification of OPMF by consecutive superheated steam and alkali treatments
The previously superheated steam-treated OPMF was used in subsequent alkali treatment. Superheated steam-treated fiber was soaked in 2% NaOH solution for 3 h at room temperature. The weight ratio of fiber to NaOH solution was fixed at 1:20. After treatment, the fiber was filtered and washed several times with water, oven-dried at 60 ˚C, and finally kept in a seal polyethylene bag for further used in analysis.

Weight Loss Analysis

The weight of fiber before and after each treatment processes were recorded using a microbalance with an accuracy of $\pm$ 0.0001 g. The percent weight loss was calculated according to the following formula,

$$Weight \quad Loss \quad (\%) \quad = \frac{W_i - W_f}{W_i} \times 100 \qquad (1)$$

where W_i is weight of fiber before treatment and W_f is weight of fiber after treatment.

Chemical Analysis

The chemical components *i.e* cellulose, hemicellulose, and lignin of fibers were determined by using the chemical analysis according to the standard procedures described by Abe *et al.* (2007). The holocellulose (combination of cellulose and hemicellulose) content of fibers was determined by gradual removal of lignin, which was achieved by treating the fibers with 5 wt% $NaClO_2$ solution at 70 $^\circ$C for 1 h, using a fiber to liquor weight ratio of 1:20. The pH of the solution was adjusted to 4 with the usage of H_2SO_4 solution. The solid residue was then filtered and washed then oven-dried at 60 $^\circ$C until constant weight was achieved. The cellulose content was determined by treating the holocellulose with 6 wt% potassium hydroxide solution for 24 h at 25 $^\circ$C. The solid residue was then filtered, washed, and oven-dried at 60 $^\circ$C until constant weight was achieved. The hemicellulose content was determined from the difference between holocellulose and cellulose contents of the fibers. To determine the lignin content, the fibers were dipped in the 72% H_2SO_4 solution at temperature of 30 $^\circ$C for 1 h, followed by dilution to 3% acid concentration and continue to reflux for 2 h. The insoluble residue was filtered, washed, and oven-dried at 60 $^\circ$C until constant weight was obtained. For moisture content determination, a weighed quantity of fibers was placed in an oven at the temperature of 105 $^\circ$C for 4 h. The weight of oven-dried fibers was then measured. The difference in their weight was corresponded to the moisture content of the fibers. Ash content was determined by heating the fibers in the furnace at temperature of 550 $^\circ$C for 2 h. The fibers were then cooled in a desiccator and finally weighed to obtain their ash content. The average values of three samples were recorded.

Fourier Transform Infrared (FTIR) Spectroscopy

The functional groups, types of bonding and chemical components in fibers were identified using a Perkin Elmer Spectrum 100 series Spectrophotometer equipped with attenuated total reflectance (ATR). The FTIR spectra of the fibers were recorded in the range of frequency of 400 to 4000 cm^{-1} with 16 scans in each case at a resolution of 4 cm^{-1}.

X-Ray Diffraction (XRD) Analysis

The degree of crystallinity for fibers was determined using a Shimadzu XRD 6000 Diffractometer with nickel filtered Cu Kα (λ = 0.1542 nm) beam operated at 30 kV and 30 mA. The fibers were scanned at 2θ range of 10 to 30° with scanning rate of 2°/min at 25 $^\circ$C. The crystallinity index (CrI) was calculated from the XRD data and determined based on the Eq. 2 (Segal *et al.* 1959),

$$CrI \; (\%) = \frac{I_{002} - I_{am}}{I_{002}} \times 100 \qquad (2)$$

where I_{002} was the maximum intensity of diffraction of the (002) lattice peak at a 2θ of 22-23° and I_{am} is the intensity of diffraction of the amorphous material, which was taken at a 2θ of 18° where the intensity is at a minimum.

Thermogravimetric Analysis (TGA)

The thermal degradation behavior of fibers was studied using a Perkin Elmer Pyris 7 TGA analyzer in the temperature range of 35 to 500 °C at a constant heating rate of 10 °C/min and continuous nitrogen flow of 20 mL/min. The sample weight used was of 10 to 15 mg. The weight loss of fibers was recorded as a function of temperature.

Scanning Electron Microscopy (SEM)

The microstructures of fibers were observed using a JEOL JSM-6400 scanning electron microscope operated at 15 kV accelerating voltage. The oven-dried fibers were placed on the metal holder and coated with gold by a Bio-rad coating system for 3 min to ensure good conductivity prior to analysis.

Water Absorption

Fibers were oven-dried at 60 °C until constant weight was obtained prior to testing. The weight of dried fibers (W_0) was measured using a microbalance with an accuracy of $\pm$ 0.0001 g. The fibers were then dipped in distilled water for 24 h at 25 °C. After dipping in water for 24 h, the fibers were removed from the distilled water and weighed immediately to obtain the wet weight (W_{24h}). The test was performed in duplicate and their average values were reported. The moisture absorption of the fibers was calculated using Eq. 3,

$$Water \quad Absorption \quad (\%) = \frac{W_{24h} - W_0}{W_0} \times 100 \qquad (3)$$

RESULTS AND DISCUSSION

The main objective of this work was to investigate the influence of various treatment processes on the chemical compositions, surface morphology, crystallinity, thermal degradation, and water absorption of OPMF. For convenience, the terms S, N, and SN in the subsequent sections are referred to superheated steam, alkali, and consecutive superheated steam-alkali treatments, respectively. Meanwhile, the terms SOPMF, NOPMF, and SNOPMF are assigned to S-, N-, and SN-treated OPMFs, respectively.

Physical Appearances

The physical appearances of untreated and treated fibers are illustrated in Fig. 1. As can be seen, the colour of the fiber was changed as a result of the treatments. As shown in Fig. 1a, OPMF had a light brown colour. The N treatment did not alter the colour of fiber, as NOPMF showed very similar colour to that of OPMF. In contrast, the S treatment produced fiber (SOPMF) with relatively dark brown colour. However, there

is no significant colour change was observed for consecutive SN treatment (SNOPMF). The change in colour of fiber upon treatments is related to the degradations of cellulose, hemicellulose, and lignin substances (Bledzki *et al.* 2010). The degradation process is normally accompanied by weight loss and alteration of chemical compositions of fiber, which will be further discussed in the subsequent section.
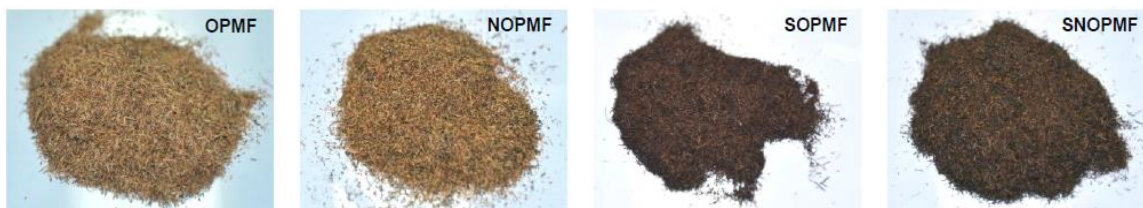

Fig. 1. Photographs OPMF, NOPMF, SOPMF, and SNOPMF

Weight Loss Analysis

The weight loss and chemical compositions change of fiber after treatments can be used as an important indicator to understand the effectiveness of each treatment process. As shown in Table 1, the weight loss of fiber after treatments increased in the sequence of NOPMF < SOPMF < SNOPMF. The NOPMF, SOPMF, and SNOPMF showed weight losses of 10.16, 15.39, and 27.65%, respectively. The weight loss after treatment is caused by the elimination of impurities and non-cellulose substances as they are sensitive to alkali and heat treatments (Bledzki *et al.* 2010). This can be further confirmed by chemical analysis of fibers in the following section. SOPMF showed higher value of weight loss relative to NOPMF as both moisture removal as well as degradations of impurities, and non-cellulose substances occurred simultaneously at high temperature. The weight loss of SNOPMF was almost two-fold of SOPMF and its value was the highest among the treated fibers. This indicates that consecutive SN treatment process imparted higher weight loss relative to single treatment process (S or N), therefore, relating to the increase in the efficiency of treatment.

Table 1. Mass Loss of Fibers After Treatment

Fibers	Weight loss (%)
OPMF	-
NOPMF	10.16
SOPMF	15.39
SNOPMF	27.65

Chemical Analysis

The chemical compositions of untreated and treated fibers are tabulated in Table 2. The major chemical components of OPMF are cellulose (32.22%), hemicellulose (31.62%), and lignin (23.89%). It is reported that the thermal and chemical resistance of hemicellulose are relatively low in comparison to those of cellulose and lignin due to its branch and amorphous structures (Wang *et al.* 2009). Therefore, hemicellulose is always the first component to be eliminated upon treatment. This was demonstrated clearly in this work. As shown in Table 2, the treated fibers showed relatively low percentage of hemicellulose but high percentages of cellulose and lignin as compared to that of untreated OPMF. This indicates that S, N, and consecutive SN treatments can selectively eliminate hemicellulose component, thereby increasing the percentages of lignin and

cellulose. Similar observation was also reported by other researchers (Bahrin *et al.* 2012) in superheated steam-treated oil palm empty fruit bunch fiber.

In this work, the percentage of hemicellulose in fibers was decreased in the order of OPMF > NOPMF > SOPMF > SNOPMF, whereas the percentages of cellulose and lignin increased in the sequence of OPMF < NOPFM < SOPMF < SNOPMF. Among the treated fibers, SNOPMF showed the lowest percentage of hemicellulose, indicating that the consecutive SN treatment process was more efficient in the removal of hemicellulose relative to N and S treatments. This observation helps to explain the higher weight loss of SNOPMF than those of NOPMF and SOPMF, as shown previously in the weight loss analysis. It is known that hemicellulose is the most hydrophilic component in fiber and is responsible for moisture absorption, whereas lignin is more hydrophobic than those of hemicellulose and cellulose. Therefore, the increase in percentage of lignin but decrease in percentage of hemicellulose in treated fiber made them more resistant to moisture absorption. This was shown clearly by relatively low moisture content of treated fibers in comparison to that of untreated fiber. Among the treated fibers, SNOPMF showed the least moisture content (2.49%) as it contained a minimal percentage of hemicellulose but a maximal percentage of lignin. Additionally, the relatively high percentage of lignin in treated fibers also gives treated fiber with relatively high ash content as compared to that of untreated fiber. This can be explained by the relatively high thermal resistance of lignin in comparison to those of hemicellulose and cellulose.

The relatively high cellulose percentage in treated fibers is beneficial in fabrication of biocomposites as the strength of cellulose is much higher than those of hemicellulose and lignin. Additionally, increasing percentage of cellulose in treated fibers can also contribute to the increase in thermal stability of the corresponding biocomposite. Moisture content in fiber is also one of the critical factors that influence the final properties of biocomposite. Generally, low moisture content of treated fibers is of importance as it can inhibit the formation of microvoids due to excessive evaporation of moisture during biocomposite fabrication, which normally gives biocomposites with undesired properties.

Table 2. Chemical Compositions of Fibers

Fibers	Cellulose (%)	Hemicellulose (%)	Lignin (%)	Moisture (%)	Ash (%)
OPMF	32.22 ± 1.54	31.62 ± 0.46	23.89 ± 1.12	7.87 ± 0.70	4.40 ± 0.60
NOPMF	38.39 ± 0.97	26.16 ± 1.21	23.68 ± 0.74	5.70 ± 0.32	6.07 ± 0.22
SOPMF	42.54 ± 0.84	18.73 ± 0.87	28.26 ± 0.68	3.74 ± 0.45	6.73 ± 0.32
SNOPMF	47.52 ± 0.98	5.27 ± 1.43	36.82 ± 0.46	2.49 ± 0.24	7.90 ± 0.45

Fourier Transform Infrared (FTIR) Spectroscopy

The functional group, type of bonding, as well as the chemical components of fibers can be identified using FTIR spectroscopy. Figure 2 shows the FTIR spectra of OPMF, NOPMF, SOPMF, and SNOPMF. The spectrum of OPMF shows its characteristic peaks at 3391 cm^{-1} (O-H stretching in cellulose and hemicellulose), 2925 and 2853 cm^{-1} (C-H stretching in cellulose and hemicellulose) (Wang *et al.* 2009), 1730 cm^{-1} (C=O stretching of the carbonyl groups in hemicellulose and/or lignin) (Sreekala *et al.* 2000), 1645 cm^{-1} (O-H bending in absorbed water) (Hosseinaei *et al.* 2012), 1514 cm^{-1} (C=C stretching of aromatic ring in lignin) (Xiao *et al.* 2001), 1434 cm^{-1} (C-H bending in crystalline cellulose) (Wang *et al.* 2009), 1245 cm^{-1} (C-O vibration of esters, ethers and

bioresources.com

phenol groups in waxy substances or C-O stretching of the acetyl groups in hemicellulose) (Herrera-Franco and Valadez-Gonzalez 2005; Sinha and Rout 2009), 1033 cm^{-1} (C-O, C-C or C-OH bending in hemicellulose) (Kacurakova *et al.* 1994), and 899 cm^{-1} (C-H bending and –CH$_2$ stretching in amorphous cellulose) (Qu *et al.* 2010). The spectra of NOPMF, SOPMF, and SNOPMF show relatively low absorbance of a peak at 3391 cm^{-1} due to the breaking of hydrogen bond between O-H groups of cellulose and hemicellulose (Saha *et al.* 2010). The decrements in absorbance of peaks at 2925, 2853, 1245, and 1033 cm^{-1} in FTIR spectra of treated fibers demonstrate the partial removal of hemicellulose and waxy substances during the treatment process. The intense peak at 1730 cm^{-1} as seen in OPMF spectrum disappeared in the spectrum of NOPMF or showed very low absorbance in the spectra of SOPMF and SNOPMF. This is attributed to the elimination of hemicellulose after treatment. This result was in line with the chemical analysis result. The low absorbance of peak at 1645 cm^{-1} indicated a reduction in a hygroscopicity of fiber after treatment. The absorbance of peak at 899 cm^{-1} in treated fibers was relatively low due to the removal of amorphous cellulose. However, the characteristic peaks of crystalline cellulose and lignin as seen at 1434 and 1514 cm^{-1}, respectively remained unaffected after treatment. Those unaffected cellulose and lignin may impede mechanical strength and hydrophobicity in treated fibers (Sinha and Rout 2009), which are of importance in manufacturing of biocomposites.
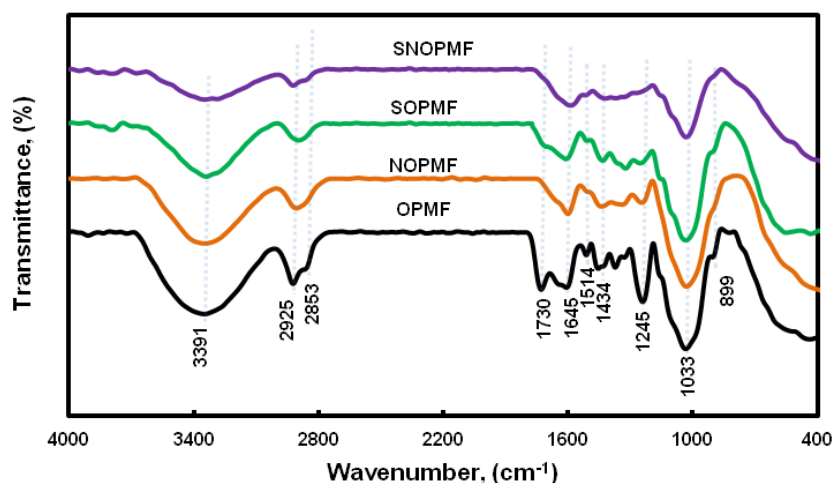

Fig. 2. FTIR spectra of OPMF, NOPMF, SOPMF, and SNOPMF

X-Ray Diffraction (XRD) Analysis

The XRD analysis was used to quantify the degree of crystallinity of the fiber after each treatment process. Figure 3 shows the XRD diffractograms of OPMF, NOPMF, SOPMF, and SNOPMF. Both untreated and treated fibers showed similar XRD patterns with two diffraction peaks at 2θ of 16.5 (101) and 22.1° (002), which correspond to amorphous and crystalline parts of fiber respectively (Segal *et al.* 1959) and are typical diffraction peaks for cellulose I (John and Thomas 2008). The diffraction peak at 16.5° was broader than that of 22.1° due to its amorphous character. The treatments did not induce any transformation of the cellulose crystal structure, as no formation of new peaks or shifting of peaks were observed in the XRD diffractograms of treated fibers. This is consistent with the result reported by Joonobi *et al.* (2010).
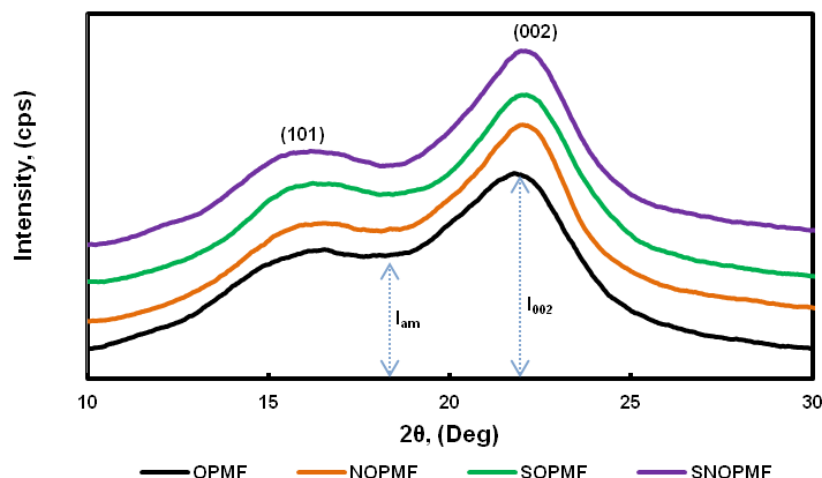
Fig. 3. XRD patterns of OPMF, NOPMF, SOPMF, and SNOPMF

As shown in Table 3, the intensities of peaks at 2θ of 18 (I_{am}) and 22.1° (I_{002}) were changed after treatments, suggesting the treatments had induced a crystallinity change of fiber. The calculated crystallinity indexes of OPMF, NOPMF, SOPMF, and SNOPMF were 33.0, 42.4, 39.7, and 45.6%, respectively. It shows that the crystallinity index of treated fibers was relatively higher than that of untreated fiber. Sinha and Rout (2009) also reported a similar observation. The increase in CrI can be attributed to the partial removal of cementing amorphous components, which mainly consist of impurities and non-cellulose substances, during the treatment processes (Joonobi *et al.* 2010). NOPMF showed higher CrI than that of SOPMF, as NaOH is able to access larger area of fiber and therefore destroy more of the amorphous region. Among the treated fibers, SNOPMF had the highest CrI due to the fact that consecutive SN treatment was more efficient to remove the cementing amorphous components, thus leading to a more compact arrangement of fiber. This result is concurrent with the chemical analysis and FTIR results. The treated fibers with relatively high crystallinity are beneficial in fabrication of biocomposites as they can improve the mechanical properties of the corresponding biocomposites (Rosa *et al.* 2012).

Table 3. Crystallinity Index of Fibers

Fibers	I_{am} (cps)	I_{002} (cps)	CrI (%)
OPMF	348	519	33.0
NOPMF	375	651	42.4
SOPMF	382	633	39.7
SNOPMF	355	653	45.6

Scanning Electron Microscopy (SEM)

Scanning electron microscopy (SEM) is an excellent technique to study the surface morphology of fiber upon various treatment processes. It could provide vital information on the degree of interfacial contact and adhesion between fiber and thermoplastic during biocomposite preparation.

The SEM micrographs of OPMF, NOPMF, SOPMF, and SNOPMF with low (300x) and high (500x) magnifications are shown in Fig. 4. OPMF is present as fiber bundles in nature, and each fiber bundle is made up of many microfibers that are bonded

bioresources.com

together by hemicellulose and lignin. The external surface of OPMF bundle seems to be wrapped by a layer of non-cellulose substances with some impurities attached on its surface (as illustrated in Figs. 4a, b.) Significant differences in the fiber surface morphologies are noted after S, N, and consecutive SN treatments. The surfaces of treated fibers appear to be relatively clean and rough in comparison to that of untreated fiber which attributes to partial the elimination of impurities as well as non-cellulose substances. This observation is similar to other reports (Mohd Edeerozey *et al.* 2007; Ibrahim *et al.* 2010). Additionally, the partial removal of those impurities and non-cellulose substances during treatment gradually revealed the silica particles (Fig. 4 d, f) that were previously embedded in the fiber bundle. It is noticeable that some of these silica particles had been removed, leaving micropores on the surface of treated fibers. In both micrographs of NOPMF and SOPMF, there were still small portions of impurities that remain on their surfaces, indicating that the N and S treatments were ineffective in removing all of the impurities from the OPMF surface.

Figures 6g and h present the SEM micrographs of SNOPMF. It can be observed that the surface of SNOPMF appears to be relatively free from impurities and silica particles. This result indicates that consecutive SN treatment was more efficient than those of N and S treatments in removing impurities as well as silica particles. Upon closer examination, the microfibers are also seen on the surfaces of SOPMF and SNOPMF, but not in NOPMF. This may be attributed to the great reduction in hemicellulose portion of SOPMF and SNOPMF, as reported earlier in the chemical analysis. This can contribute to the separation of fiber bundle and subsequently lead to the exposure of microfibers that are previously bonded together by hemicellulose and lignin. A similar observation was also reported by Joonobi *et al.* (2010) in bleached kenaf fiber.

The relatively clean, porous, rough, and texture surfaces of treated fibers are advantageous for natural fiber-thermoplastic adhesion as it can facilitate both mechanical interlocking and the bonding reaction (Abdul Razak *et al.* 2014). Additionally, the presence of microfibers is also beneficial for biocomposite fabrications, as it can increase the available area for contact between natural fibers and thermoplastic, hence their interfacial adhesion would be expected to improve (Razera *et al.* 2004).

Thermogravimetric Analysis (TGA)

Thermogravimetric analysis is performed to understand the degradation behaviors of the untreated and treated fibers, which is important during the processing of the fibers into biocomposites. Untreated natural fiber normally has low thermal resistance and tends to degrade during compounding by releasing of unpleasant smell. Some of these degraded products can be trapped inside the biocomposite and result in the formation of microvoids. This may lead to biocomposite with undesired properties.

Previous works reported that the degradation process of natural fiber can be divided into four individual stages, namely moisture evaporation, followed by hemicellulose, cellulose, and lignin decompositions, which are fall within temperature ranges of 35-160, 220-315, 315-400, and 160-900 °C, respectively (Yang *et al.* 2007). The degradation temperature of lignin is overlapped with those of cellulose and hemicellulose degradation. This is caused by the complex structure of lignin, which contains various oxygen-containing functional groups with various thermal degradation behaviors (Brebu and Vasile 2010).
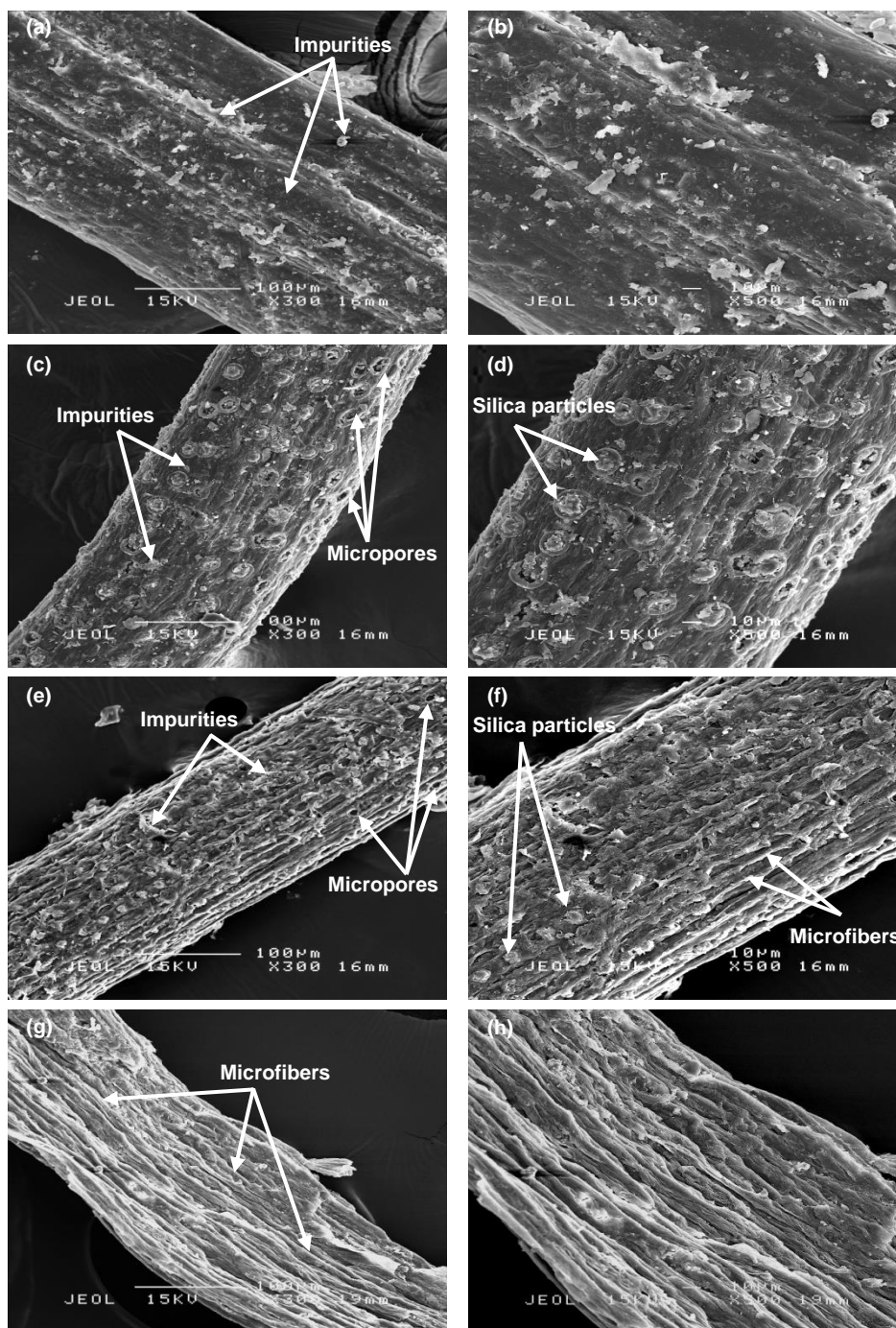
Fig. 4. SEM micrographs of OPMF (a, b), NOPMF (c, d), SOPMF (e, f) and SNOPMF (g, h)

The thermogravimetric (TG) and derivative thermogravimetric (DTG) curves of OPMF, NOPMF, SOPMF, and SNOPMF are graphically displayed in Figs. 5a and b, respectively. The TG curves (Fig. 5a) show multiple degradation steps due to the sequential degradation of different components in fibers. This is clearly illuminated in DTG curves (Fig. 5b) where three distinguishable peaks are observed over the temperature range of studied. The first peak as seen in DTG curves is assigned to moisture evaporation as well as degradation of low molecular weight substances, the second peak to hemicellulose degradation, and the third peak to cellulose degradation.

The peak height at each thermal degradation stage as observed in DTG curves can be used as an indicator to estimate the relative amount of each component presence in fibers. The details on the weight loss of fibers at each thermal degradation stage as well as its residue at 500 ˚C are tabulated in Table 4.
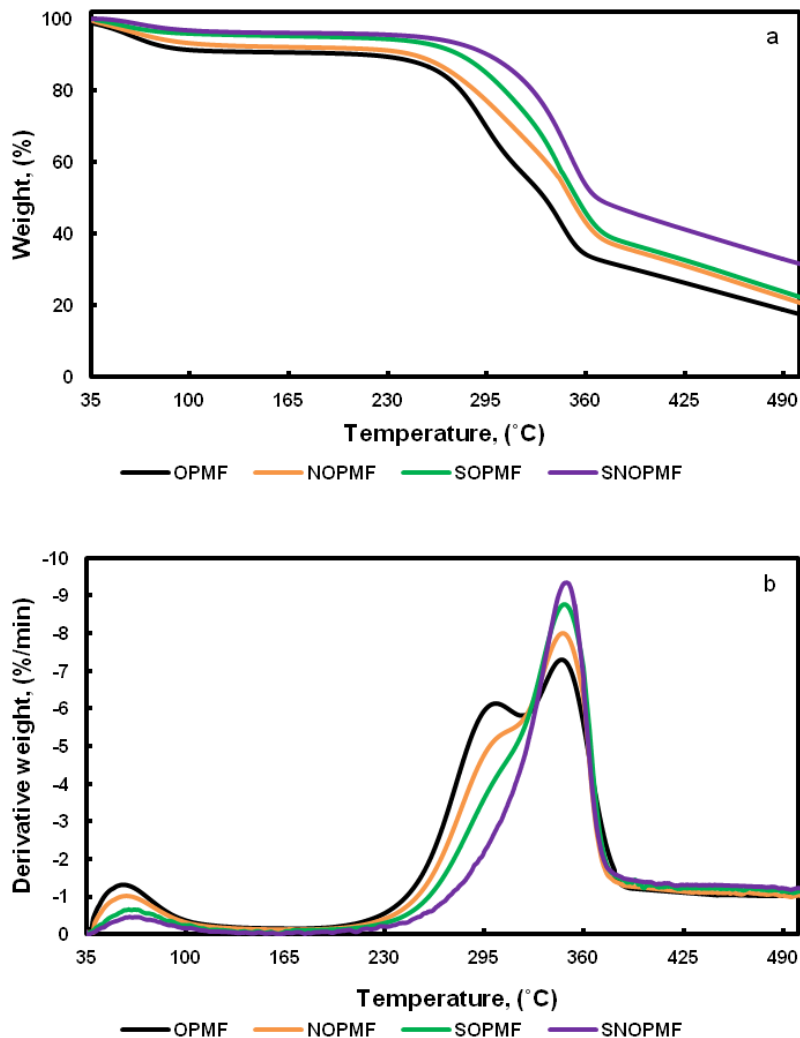

Fig. 5. TG (a) and DTG (b) curves of fibers

Table 4. Weight Loss of Fibers and Their Residue at 500 ˚C

Sample	Weight loss, (%)			Residue at 500 ˚C, (%)
	35-160 ˚C	160-315 ˚C	315-500 ˚C	
OPMF	9.33	32.20	40.87	17.60
NOPMF	7.73	23.56	47.98	20.73
SOPMF	4.47	19.24	53.89	22.40
SNOPMF	3.94	11.78	52.71	31.57

Generally, the treated fibers showed relatively low levels of moisture evaporation or volatile products (3.94 to 7.73%) as compared to that of untreated fiber (9.33%), which can be found by the weight loss in the temperature range of 35 to 160 ˚C (Rosa *et al.* 2012). As the temperature is increased from 160 to 315 ˚C, another derivative peak was

observed with maximum rate of weight loss which occurred at around 298.21 °C. This degradation stage is attributed mainly to the deacetylation of hemicellulose to form acetic acid (Hosseinaei *et al.* 2012). Also, NOPMF (23.56%), SOPMF (19.24%), and SNOPMF (11.78%) showed relatively low value of weight loss as compared to that of OPMF (32.20%). This is in accordance with the chemical analysis and FTIR results previously shown. Further increase in temperature from 315 to 500 °C has led to the glycosidic bonds breakage of cellulose as well as degradation of lignin (Sinha and Rout 2009; Bledzki *et al.* 2010; Gu *et al.* 2013). A derivative peak was seen at a temperature of 342.63 °C due to maximum rate of weight loss for cellulose. This temperature is close to the value (348 °C) reported by Moran *et al.* (2008) for commercial cellulose. In the current stage, the weight loss value of treated fibers (47.98 to 52.71%) was higher relative to that of OPMF (40.87%). This can be explained by the increasing percentages of cellulose and lignin in treated fibers. At 500 °C, the residue in treated fibers appeared to be higher than that of OPMF, attributing to the high percentage of lignin in treated fibers. This result is corroborated with earlier statement as reported in chemical analysis.

The thermal degradation temperature of fibers at 5, 10, and 50% weight loss is tabulated in Table 5. Generally, the treated fibers showed higher degradation temperature relative to OPMF. For instance, the degradation temperature at 10% weight loss ($T_{10\%}$) of OPMF was 215.42 °C, and 247.44, 277.44, and 295.26 °C for NOPMF, SOPMF, and SNOPMF, respectively. It is known that after the treatment process, the treated fibers are comprised of increasing percentages of cellulose and lignin due to the elimination of hemicellulose. The cellulose and lignin are more thermally stable relative to hemicellulose. Therefore, the relatively high percentages of lignin and cellulose in treated fibers made it difficult to decompose and subsequently increased their thermal stability. The increase in thermal stability of treated fibers is beneficial in processing the treated fibers into biocomposites.

Table 5. Thermal Degradation Temperature of Fibers at 5, 10, and 50% Weight Loss

Sample	Temperature °C		
	$T_{5\%}$	$T_{10\%}$	$T_{50\%}$
OPMF	63.46	215.42	332.98
NOPMF	75.63	247.44	350.23
SOPMF	198.09	277.44	354.11
SNOPMF	249.14	295.26	367.24

Water Absorption

One of the disadvantages of natural fiber that can make it unsuitable for biocomposite applications is its hygroscopic behavior. It tends to absorb moisture once exposed to humid environment, and this often results in biocomposite with undesired properties. Therefore, the hygroscopicity of natural fiber should be reduced in order to make it more suitable for biocomposite applications. The water absorption (WA) of OPMF, NOPMF, SOPMF, and SNOPMF after 24 h of immersion in water is shown in Fig. 6. Both untreated and treated fibers showed increase in water absorption after 24 h of immersion in water. This can be attributed to the presence of accessible hydroxyl groups in fiber, which facilitate hydrogen bonding with water molecules and subsequently increase the water absorption (Islam *et al.* 2010; Ahmad Thirmizir *et al.* 2011). However, the treated fibers show relatively low WA as compared to that of untreated fiber. This can

be explained by the decrease in the amount of hydroxyl groups accessible to water absorption as hemicellulose is eliminated partially by N, S, and consecutive SN treatments. The untreated OPMF shows WA of 139.11% and it was reduced to 122.28, 105.98, and 76.29% for NOPMF, SOPMF, and SNOPMF, respectively. SNOPMF shows almost two fold reductions in WA as compared to that of untreated OPMF, indicating consecutive SN treatment is more prominent to produce fiber with relatively high water resistance. The reduction in hygroscopicity of fiber after treatments could increase its suitability to be used in biocomposite fabrications.
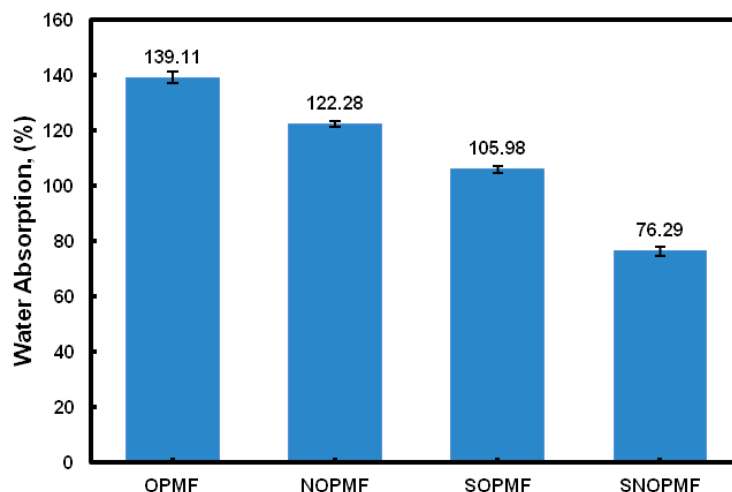

Fig. 6. Water absorption of OPMF, NOPMF, SOPMF, and SNOPMF

CONCLUSIONS

1. The properties of OPMF were successfully modified by means of alkali, superheated steam, and consecutive superheated steam-alkali treatments.

2. The percentages of cellulose and lignin in fiber were found to be increased after alkali, superheated steam, and consecutive superheated steam-alkali treatments due to the elimination of hemicellulose, as validated by FTIR spectroscopy and chemical analysis.

3. The surface of treated fibers became relatively clean and rough in texture after treatments due to the removal of impurities and non-cellulose substances. Microfibers were also seen in superheated steam- and consecutive superheated steam-alkali-treated fibers, which was attributed to the partial separation of fiber bundle.

4. The crystallinity index and thermal stability of treated fibers were relatively higher due to the removal of impurities and hemicellulose, which consisted mainly of amorphous materials with relatively low thermal resistance.

5. The hygroscopicity of fiber was reduced after alkali, superheated steam, and consecutive superheated steam-alkali treatments.

6. The consecutive superheated steam-alkali treatment was a more efficient treatment process relative to alkali or superheated steam treatment.

ACKNOWLEDGMENTS

REFERENCES CITED

Abdul Razak, N. I., Ibrahim, N. A., Zainuddin, N., Rayung, M., and Saad, W. Z. (2014). "The influence of chemical surface modification of kenaf fiber using hydrogen peroxide on the mechanical properties of biodegradable kenaf fiber/poly(lactic acid) composites," *Molecules* 19(3), 2957-2968. DOI: 10.3390/molecules19032957

Abe, K., Iwamoto, S., and Yano, H. (2007). "Obtaining cellulose nanofibers with a uniform width of 15 nm from wood," *Biomacromolecules* 8(10), 3276-3278. DOI: 10.1021/bm700624p

Ahmad Thirmizir, M. Z., Mohd Ishak, Z. A., Taib, R. M., Rahim, S., and Mohamad Jani, S. (2011). "Kenaf-bast-fiber-filled biodegradable poly(butylene succinate) composites: effects of fiber loading, fiber length, and maleated poly(butylene succinate) on the flexural and impact properties," *Journal of Applied Polymer Science* 122(5), 3055-3063. DOI: 10.1002/app.34046

Bahrin, E. K., Baharuddin, A. S., Ibrahim, M. F., Abdul Razak, M. N., Sulaiman, A., Abd-Aziz, S., Hassan, M. A., Shirai, Y., and Nishida, H. (2012). "Physicochemical properties changes and enzymatic hydrolysis enhancement of oil palm empty fruit bunches treated with superheated steam," *BioResources* 7(2), 1784-1801. DOI: 10.15376/biores.7.2.1784-1801

Bledzki, A. K., Mamun, A. A, and Volk, J. (2010). "Physical, chemical and surface properties of wheat husk, rye husk and soft wood and their polypropylene composites," *Composites Part A: Applied Science and Manufacturing* 41(4), 480-488. DOI: 10.1016/j.compositesa.2009.12.004

Brebu, M., and Vasile, C. (2010). "Thermal degradation of lignin—A review," *Cellulose Chemistry and Technology* 44(9), 353-363.

GGS. (2014). *Global Green Synergy Sdn Bhd: Biomass*, (http://www.ggs.my/index.php/biomass/biomass-in-palm-industry).

Gu, X. L., Ma, X., Li, X. L., Liu, C. A., Cheng, K. H., and Li, Z. (2013). "Pyrolysis of poplar wood sawdust by TG-FTIR and Py-GC/MS," *Journal of Analytical and Applied Pyrolysis* 102, 16-23. DOI: 10.1016/j.jaap.2013.04.009

Herrera-Franco, P. J., and Valadez-Gonzalez, A. (2005). "A study of the mechanical properties of short natural-fiber reinforced composites," *Composites Part B: Engineering* 36(8), 597-608. DOI: 10.1016/j.compositesb.2005.04.001

Hosseinaei, O., Wang, S., Enayati, A. A., and Rials, T. G. (2012). "Effects of hemicellulose extraction on properties of wood flour and wood-plastic composites," *Composites Part A: Applied Science and Manufacturing* 43(4), 686-694. DOI: 10.1016/j.compositesa.2012.01.007

Ibrahim, N. A., Hadithon, K. A., and Abdan, K. (2010). "Effect of fibre treatment on mechanical properties of kenaf-Ecoflex composites," *Journal of Reinforced Plastics and Composites* 29(14), 2192-2198. DOI: 10.1177/0731684409347592

Islam, M. N., Rahman, M. R., Haque, M. M., and Huque, M. M. (2010). "Physico-mechanical properties of chemically treated coir reinforced polypropylene composites," *Composites Part A: Applied Science and Manufacturing* 41(2), 192-198. DOI: 10.1016/j.compositesa.2009.10.006

John, M. J., and Thomas, S. (2008). "Biofibres and biocomposites," *Carbohydrate Polymers* 71(3), 343-364. DOI: 10.1016/j.carbpol.2007.05.040

Joonobi, M., Harun, J., Tahir, P., Zaini, L., Saiful, A. S., and Makinejad, M. (2010). "Characteristics of nanofibers extracted from kenaf core," *BioResources* 5(4), 2556-2566. DOI: 10.15376/biores.5.4.2556-2566

Kacurakova, M., Ebringerova, A., Hirsch, J., and Hromadkova, Z. (1994). "Infrared study of arabinoxylans," *Journal of the Science of Food and Agriculture* 66(3), 423-427. DOI: DOI: 10.1002/jsfa.2740660323

Kalia, S., Kaith, B. S., and Kaur, I. (2009). "Pretreatments of natural fibers and their application as reinforcing material in polymer composites – A review," *Polymer Engineering & Science* 49(7), 1253-1272. DOI: 10.1002/pen.21328

Lau, H. L. N., Choo, Y. M., Ma, A. N., and Chuah, C. H. (2008). "Selective extraction of palm carotene and vitamin E from fresh palm-press mesocarp fiber (*Elaeis guineensis*) using supercritical CO_2," *Journal of Food Engineering* 84(2), 289-296. DOI: 10.1016/j.jfoodeng.2007.05.018

Mohd Edeerozey, A. M., Hazizan, M. A., Azhar, A. B., and Zainal Ariffin, M. I. (2007). "Chemical modification of kenaf fibers," *Materials Letters* 61(10), 2023-2025. DOI: 10.1016/j.matlet.2006.08.006

Moran, J. I., Alvarez, V. A., Cyras, V. P., and Vazquez, A. (2008). "Extraction of cellulose and preparation of nanocellulose from sisal fibers," *Cellulose* 15(1), 149-159. DOI: 10.1007/s10570-007-9145-9

Mwaikambo, L. Y., and Ansell, M. P. (2002). "Chemical modification of hemp, sisal, jute, and kapok fibers by alkalization," *Journal of Applied Polymer Science* 84(12), 2222-2234. DOI: 10.1002/app.10460

Qu, P., Gao, Y., Wu, G., and Zhang, L. (2010). "Nanocomposites of poly(lactic acid) reinforced with cellulose nanofibrils," *BioResources* 5(3), 1811-1823. DOI: 10.15376/biores.5.3.1811-1823

Rayung, M., Ibrahim, N. A., Zainuddin, N., Saad, W. Z., Abdul Razak, N. I., and Chieng, B. W. (2014). "The effect of fiber bleaching treatment on the properties of poly(lactic acid)/oil palm empty fruit bunch fiber composites," *International Journal of Molecular Sciences* 15(8), 14728-14742. DOI: 10.3390/ijms150814728

Razera, I. A. T., and Frollini, E. (2004). "Composites based on jute fibers and phenolic matrices: Properties of fibers and composites," *Journal of Applied Polymer Science* 91(2), 1077-1085. DOI: 10.1002/app.13224

Rosa, S. M. L., Rehman, N., De Miranda, M. I. G., Nachtigall, S. M. B., and Bica, C. l. D. (2012). "Chlorine-free extraction of cellulose from rice husk and whisker isolation," *Carbohydrate Polymers* 87(2), 1131-1138. DOI: 10.1016/j.carbpol.2011.08.084

Saha, P., Manna, S., Chowdhury, S. R., and Sem, R. (2010). "Enhancement of tensile strength of lignocellulosic jute fibers by alkali-steam treatment," *Bioresource Technology* 101(9), 3182-3187. DOI: 10.1016/j.biortech.2009.12.010

Segal, L., Creely, J. J., Martin Jr, A. E., and Conrad, C.M. (1959). "An empirical method for estimating the degree of crystallinity of native cellulose using X-ray

diffractometer," *Textile Research Journal* 29(10), 786-794. DOI: 10.1177/004051755902901003

Sinha, E., and Rout, S. K. (2009). "Influence of fibre-surface treatment on structural, thermal and mechanical properties of jute fibre and its composite," *Bulletin of Materials Science* 32(1), 65-76. DOI: 10.1007/s12034-009-0010-3

Sreekala, M. S., Kumaran, M. G., and Thomas, S. (1997). "Oil palm fibers: Morphology, chemical composition, surface modification, and mechanical properties," *Journal of Applied Polymer Science* 66(5), 821-835. DOI: 10.1002/(SICI)1097-4628(19971031)66:5<821::AID-APP2>3.0.CO;2-X

Sreekala, M. S., Kumaran, M. G., Joseph, S., and Jacob, M. (2000). "Oil palm fibre reinforced phenol formaldehyde composites: Influence of fibre surface modifications on the mechanical performance," *Applied Composite Materials* 7(5–6), 295-329. DOI: 10.1023/A:1026534006291

Teh, C. C., Ibrahim, N. A., and Wan Yunus, W. M. Z. (2013). "Response surface methodology for the optimization and characterization of oil palm mesocarp fiber-graft-poly(butyl acrylate)," *BioResources* 8(4), 5244-5260. DOI: 10.15376/biores.8.4.5244-5260

Then, Y. Y., Ibrahim, N. A., Zainuddin, N., Ariffin, H., and Wan Yunus, W. M. Z. (2013). "Oil palm mesocarp fiber as new lignocellulosic material for fabrication of polymer/fiber biocomposites," *International Journal of Polymer Science* Vol. 2013, Article ID 797452, 7 pages. DOI: 10.1155/2013/797452

Then, Y. Y., Ibrahim, N. A., Zainuddin, N., Ariffin, H., Wan Yunus, W. M. Z., and Chieng, B. W. (2014). "The influence of green surface modification of oil palm mesocarp fiber by superheated steam on the mechanical properties and dimensional stability of oil palm mesocarp fiber/poly(butylene succinate) biocomposite," *International Journal of Molecular Sciences* 15(9), 15344-15357. DOI: 10.3390/ijms150915344

Wang, K. B., Jiang, J. X., Xu, F., and Sun, R. C. (2009). "Influence on steaming pressure on steam explosion pretreatment of Lespedeza stalks (*Lespedeza cryobotrya*): Part 1. Characteristic of degraded cellulose," *Polymer Degradation and Stability* 94(9), 1379-1388. DOI: 10.1016/j.polymdegradstab.2009.05.019

Xiao, B., Sun, X. F., and Sun, R. (2001). "Chemical, structural, and thermal characterizations of alkali-soluble lignins and hemicelluloses, and cellulose from maize stems, rye straw, and rice straw," *Polymer Degradation* and *Stability* 74(2), 307-319. DOI: 10.1016/S0141-3910(01)00163-X

Yang, H., Yan, R., Chen, H., Lee, D. H., and Zheng, C. (2007). "Characteristics of hemicellulose, cellulose and lignin pyrolysis," *Fuel* 86 (12–13), 1781-1788. DOI: 10.1016/j.fuel.2006.12.013